

PHYS 235 – Motion Beyond Brownian

Levy Stable Distributions, Fractional Kinetics, and Much More!

A Summary of Pat Diamond's Notes by Steve Molesworth – Spring 2022

Table of Contents

1	<i>Fractional Brownian Motion</i>	2
1.1	Hurst Parameter	2
1.2	Noise, Noise, Noise!	4
2	<i>Levy-Stable Distributions</i>	5
2.1	Generalizing the Central Limit Theorem	6
2.2	Taking Flight	7
3	<i>Continuous Time Random Walk</i>	10
3.1	Waiting Time Model	11
3.2	Velocity Model	12
4	<i>Fractional Kinetics</i>	13
4.1	Fractional Calculus Basics	14
4.2	Fractional Kinetic Equation	15
4.3	Weierstrass Random Walk	17
5	<i>References</i>	19

1 Fractional Brownian Motion

The reader is undoubtedly familiar with the discrete random walk and its continuous analog, Brownian motion. While these concepts describe phenomena in nature, economics, and numerous other fields, they only account for a subset of observations. Allowing for some degree of “memory” between increments leads to generalized Brownian motion where temporal intermittency, in addition to spatial like in earlier lectures, occurs and fractal behavior manifests.

1.1 Hurst Parameter

Howard Hurst desired a method of calculating optimal reservoir volume – no flooding or complete emptying – for the Aswan Dam along the Nile River. Given the large populations dependent on consistent water discharges, his design was incredibly important. Rather than assume a stationary random walk, Hurst compiled system variables measurements at regular intervals and observed large variances. Mandelbrot and Wallis later categorized the low frequency extremum in time series behavior as Noah and Joseph effects. “Joseph effects” are persistent events like seven years of abundance followed by seven years of famine, and “Noah effects” are intensely concentrated tail outcomes like the Great Flood [1]. Anomalies such as these, more recently deemed “Black Swans” by Nicholas Nassim Taleb, drove the Aswan Dam into becoming the largest embankment dam.

In opposition to typical expectation values, E , resulting from a Brownian time series step, δB ,

$$E[\delta B^2] = \tau \quad (1.1.1)$$

Mandelbrot and Ness proposed an alternative named fractional or fractal Brownian Motion,

$$E[\delta B^2] = \tau^{2H}, \quad 0 \leq H \leq 1 \quad (1.1.2)$$

where H is the Hurst exponent and τ is the time between observations [2]. This formulation captures Brownian motion and the Weiner process when $H = 1/2$, but more accurately models “persistent” ($1/2 \leq H \leq 1$) and “sticky” ($0 \leq H \leq 1/2$) systems. Other common term pairings describing these processes are wild and mild; super- and sub-diffusive; or correlated and anti-correlated. Solving (1.1.2) for H ,

$$H = \frac{\ln|\delta B|}{\ln|\tau|} \quad (1.1.3)$$

shows similarity with the box-counting dimension, $D_o = \ln|N|/\ln|1/\epsilon|$. H can therefore be interpreted as a measure of fractal dimensionality for Brownian processes. These quantities are related by

$$H + D = 1 + n, \quad n \leq H \leq n + 1 \quad (1.1.4)$$

for an n-dimensional space. The expression in (1.1.2) can be further generalized for multifractality with H dependent on scale q. Roughness or randomness in a time series thus scales with H as D does in turbulence.

$$E[\delta B^q] = \tau^{qH(q)}, 0 \leq H(q) \leq 1 \quad (1.1.5)$$

One technique for estimating the Hurst Parameter is through the “rescaled range”, R/S. Crudely, this requires calculating standard deviations, S_n , and cumulative deviates from the means for varying amounts of the entire observation series; taking the range, R_n , of said cumulative deviates; and dividing R_n by S_n . From here, one can log-log plot R_n/S_n against the number of observations in the n^{th} set and take the slope to obtain H,

$$H = \frac{\ln|R_n/S_n|}{\ln|n|} \quad (1.1.6)$$

Figure 1 shows Hurst’s plot for various phenomena [3]. At $H \sim 0.75$, rivers clearly deviate from Brownian motion! Alternatively, R/S relates to the expectations values like in (1.1.1-2),

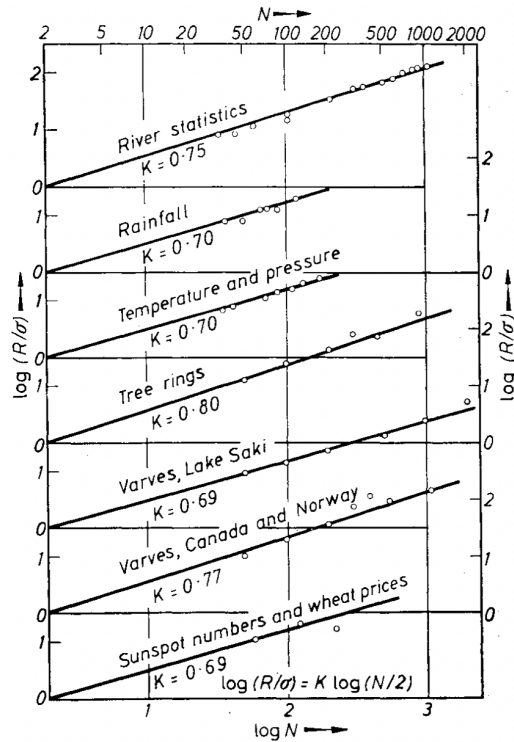


Figure 1 - R/S Plots for various time series where K is equivalent to H [3].

$$E(R_n/S_n) = Cn^H \quad (1.1.7)$$

with some constant, C, and the number of points in the series, n.

An interesting connection exists between this topic and wealth distribution across populations via the Gini coefficient, G. Expressed in terms of individual wealth x_i , the Gini coefficient is,

$$G = \frac{\sum_{i=1}^n \sum_{j=1}^n |x_i - x_j|}{2n \sum_{i=1}^n x_i} \quad (1.1.8)$$

In the limiting case where one person holds all wealth, $G=1$, but more generally G parallels R from before, and describes concentration within a series. Plotting cumulative distribution functions for perfect equality and the Lorenz curve, which resembles many real populations, the “wealth gap” – equivalent to G – appears graphically as the normalized area after subtracting curves, $A/(A+B)$ (Figure 2) [4]. Economists later measured the Gini index’s applicability in “education inequality” through level of education attained by members of a population [4]. Quality of education aside, the researchers again found large inequality gaps: Mali’s education Gini index was 0.92 in 1990 [4]!

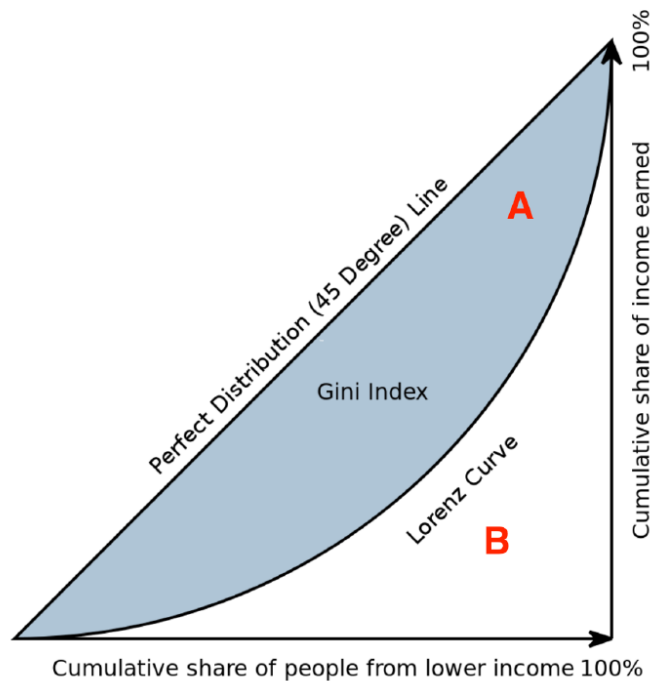


Figure 2 - Geometric Interpretation of Gini Index and Socioeconomic Inequality [4]

1.2 Noise, Noise, Noise!

“...there is noise – and more of it than you think.” – Daniel Kahneman (*Noise*, 2021)

Performing Fourier transforms on time series with inclusion of H reveals additional points for differentiation. The general expression is

$$\langle B^2(\omega) \rangle = \int_t^{t+\tau} \langle B(t)B(t+\tau) \rangle e^{i\omega\tau} d\tau \approx \omega^{-\beta} \quad (1.1.9)$$

$$\beta = 2H - 1$$

At $H=1/2$, $\langle B^2(\omega) \rangle = 1$ and the spectrum matches white noise, an expected result. As H approaches one $\langle B^2(\omega) \rangle \sim 1/\omega$ which was aptly named “1/f” noise but is more recognizable by pink noise. Power at lower frequencies dominates the spectrum since power spectral density decays with increasing frequency. Finally, H near zero means $\langle B^2(\omega) \rangle = \omega$, which is blue noise. These spectrums are depicted in Figure 3 [5]. In terms of fractal dimensionality, notice $H=0$ generates a two-dimensional curve in time matching $D=(2-H)=2$, while $H=1$ is dominated by a one-dimensional line following $D=1$.

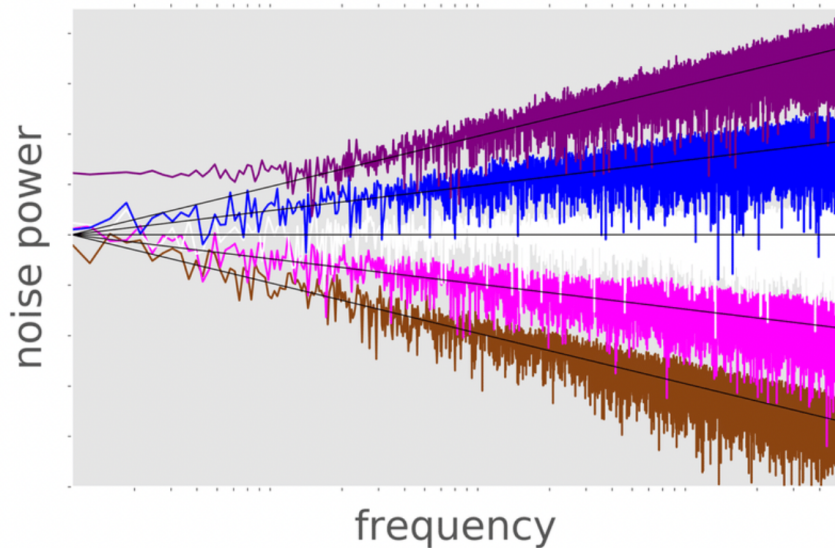


Figure 3 - The Colors of Noise [5]

The case of $1/f$ noise deserves further attention due to its pervasiveness in physical systems. First, Zipf’s law parallels $1/f$ noise when an empirical exponent, s , equals one as it approximately does for human languages. Zipf’s law relates a word’s appearance frequency, $f(k)$, to its frequency ranking, k by $f(k) \sim 1/k^s$.

2 Levy-Stable Distributions

Recognizing that non-Gaussian probability distributions arise when $H \neq 1/2$, one might question the central limit theorem’s (CLT) validity. Recall that traditional CLT asserts a sum of n random, independent, and identically distributed (IID) variables with finite, non-zero second moments, or variances, tends towards a normal distribution as $n \gg 1$ regardless of variable-specific probability density functions. The Gaussian is then an attractor in function space under these conditions. Notice no value has been assigned to higher moments: a negative kurtosis alone can cause heavy tails. Allowing for $0 \leq H \leq 1$ and infinite variance reveals a large class of stable distributions deemed Levy-stable of which the Gaussian, with $H=1/2$, is a special case with finite variance.

2.1 Generalizing the Central Limit Theorem

CLT must be proven with a twist to characterize L-stable processes. In terms of incremental steps like the previous section, begin with the Chapman-Kolmogorov equation with its usual Markovian (no memory) conditions on the steps,

$$P_N(x) = \int dy P_{N-1}(y)P_N(x|y) \quad (2.1.1)$$

This states the probability of finding a particle at position x at step N is $P_N(x)$ and is the cumulative joint probability, $P_{N-1}(y)P_N(x|y)$, of all particles in the range of y during step $N-1$ making increments along path $x-y$. Reaching step N may require a length convolution, which would be convenient to avoid, so apply the Fourier transform to convert convolutions into products:

$$P_N(k) = \prod_{n=1}^N \hat{P}_n(k) \rightarrow P_N(x) = \int dk \prod_{n=1}^N \hat{P}_n(k) e^{ikx} / 2\pi \quad (2.1.2)$$

Under IID constraints, each $\hat{P}_n(k)$, the generating function, must be equivalent, so the cumulative probability is an infinite product as $N \rightarrow \infty$.

$$\lim_{N \rightarrow \infty} \prod_{n=1}^N \hat{P}_n(k) = \hat{P}_N(k) \quad (2.1.3)$$

Applying moments, $m_n = \langle x^n \rangle$, to $\hat{P}(k)$ results in the generating function of a multiplicative, and Levy-stable, process,

$$\hat{P}(k) = \sum_{n=0}^{\infty} (-i)^n k^n m_n / n! = 1 - im_1 k - m_2 k^2 / 2 + \dots \quad (2.1.4)$$

$$F(m_n) = i^n \partial P / \partial k^n |_{k=0}$$

The existence of moments depends on existence of generating function derivatives and therefore relates to roughness. Referring to (2.1.2) and taking $\psi(k) = \ln \hat{P}(k)$ shows

$$\psi(k) = -iC_1 k - C_2 k^2 / 2 + \dots \quad (2.1.5a)$$

$$(C_1 = m_1, C_2 = m_2 - m_1^2 = \sigma^2 \dots)$$

$$P(x) = \int dk e^{ikx + \psi(k)} / 2\pi \quad (2.1.5b)$$

where C_n are the cumulants that are additive for IID, $\psi_N = N\psi(k)$. By the Laplace method and with large N , k near zero dominates (2.1.5b). Then, for a zero mean $-C_1 = 0$,

$$P_N(x) = \int dk e^{ikx - \frac{NC_2 k^2}{2}} / 2\pi = \frac{1}{2\pi\sqrt{NC_2}} e^{-\frac{x^2}{NC_2}} \quad (2.1.6)$$

and the CLT is recovered. Like before, sufficiently large N and finite C_2 drives the PDF to a Gaussian, which acts as the function space attractor, but things become more interesting when higher moments are divergent.

2.2 Taking Flight

For n IID, random, normalized variables,

$$x_{n+1} = \sum_{i=1}^n \frac{c_i x_i}{c} \quad (2.2.1)$$

and a characteristic function describing the shared probability function,

$$P(q) = \int_{-\infty}^{\infty} e^{iqx} P(x) \quad (2.2.2)$$

we can state the recursive relation:

$$P(cq) = \prod_{i=1}^n P(c_i x_i) \rightarrow \ln P(cq) = \sum_{i=1}^n \ln P(c_i x_i) \quad (2.2.3)$$

Each distribution has a scaling parameter, c_i , and they are related to the global scaling parameter, c , by $c^\alpha = \sum_{i=1}^n c_i^\alpha$. Using logarithms means a power law is afoot. The scaling parameter relation suggests $\ln P_\alpha(cq) = (cq)^\alpha$ and we arrive at the Levy- α stable distribution,

$$P_\alpha(q) = e^{-c|q|^\alpha}, \quad 0 \leq \alpha \leq 2 \quad (2.2.4)$$

This is a self-similar generating function with stability parameter α . It is equal to the Gaussian distribution when $\alpha=2$ and the Cauchy or Lorentz distribution when $\alpha=1$. Like H , α can take fractional values, which requires fractional calculus and a generalized Fokker-Planck equation to be derived later.

An equivalent result to (2.2.4) is obtained by rescaling the probability density functions and solving for a fixed function attractor in the large- n limit, $F_n(cq) \rightarrow F(q)^n$. Begin by rescaling $x = x_n/a_n$, so

$$P_n(q) = F_n(a_n q) \quad (2.2.5)$$

where F_n is the scaled PDF and c is the ‘‘global’’ rescaling parameter. Move back to a recursion problem using a variable scaling parameter, $\mu(\lambda)$,

$$F(q\mu(\lambda)) = F(q)^\lambda \quad (2.2.6)$$

and convert it to a fixed-point equation with $\psi(q) = \ln F(q)$,

$$\psi(q\mu(\lambda)) = \lambda\psi(q) \rightarrow q \frac{\partial\mu}{\partial\lambda} \frac{\partial\psi(q\mu(\lambda))}{\partial q} = \psi(q) \quad (2.2.7a)$$

$$\frac{\partial\psi(q)}{\partial q} = \frac{\psi(q)}{\frac{\partial\mu(1)}{\partial\lambda} q} \quad (\mu(1) = 1) \quad (2.2.7b)$$

The self-similarity in $\psi(q)$ is thus evident, and results in a familiar generating function,

$$F(q) \approx e^{-c|q|^\alpha}, \quad 0 \leq \alpha \leq 2 \quad (2.2.8)$$

The multiplicative process results in a normal distribution with finite variance, otherwise “fat tails” dominate and the distribution is some power law. Fat tails simply refer to divergent higher moments, often kurtosis or skewness, despite meeting the CLT, and evident by infrequent, large impact outliers. Mandelbrot claimed Pareto-Levy distributions as the most positively skewed distributions ($1 < \alpha < 2$) and are potentially familiar to the reader for their “80-20” behavior. Also, the random variable(s) satisfying a normal distribution in this context would be log-normally distributed because their logarithms are additive. Examples of such distributions are plotted in Figure 4 [6].

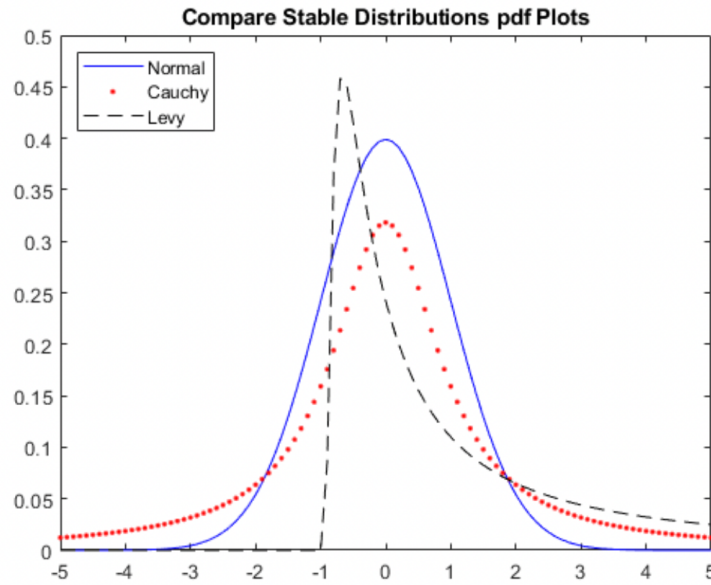


Figure 4 - Levy Stable Distribution Examples [6]

Considering a chain of distributed increments in a particle’s time-dependent walk helps bring this all back to physics. Normal step distributions cause Brownian leading to Fick-like diffusion (Figure 5, left), but the stability parameter’s range greatly alters particle motion because fat tails lead to large jumps, or flights, in Levy walks [7]. One might hear Levy or Cauchy flights depending

on the specific step distribution, but Rayleigh flights refer to normal distributions. Discretizing the Levy-stable distribution into N pieces in x ,

$$P_N(x) = \frac{1}{N^{1/\alpha}} e^{-c|x/N^{1/\alpha}|^\alpha} \quad (2.2.9)$$

where the distribution width and strength are $N^{1/\alpha}$ and c , respectively. Then, making (2.2.4) explicit in time, the characteristic function is,

$$P_\alpha(x, t) = \int dq P_\alpha(q, ct) e^{-iqx} / 2\pi \quad (2.2.10a)$$

$$\lim_{x \rightarrow \infty} P_\alpha(x, t) = t|x|^{-(\alpha+1)} \quad (2.2.10b)$$

Allowing such a walk to play out results in random walks like Figure 5 (right) [7]. Diffusion clearly varies into a ballistic regime for $\alpha > 1/2$. Notice the invariance and fractal nature under magnification as well: this is self-similarity.

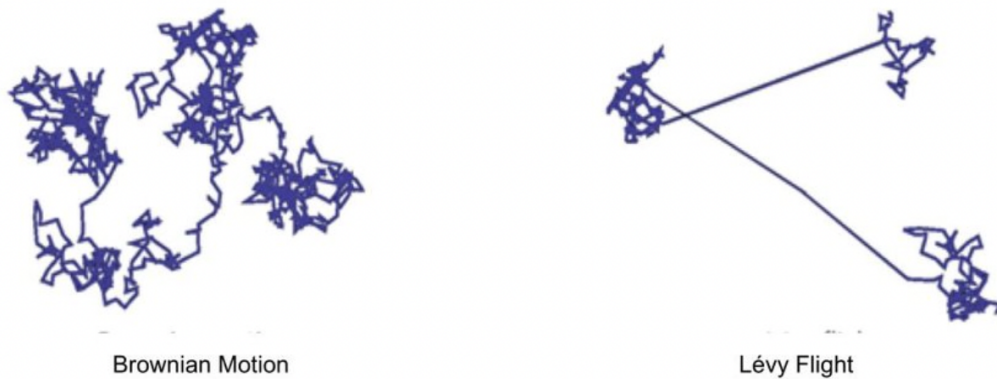


Figure 5 - Brownian (left) and Levy (right) walks [7]

Weeks and Swinney reported experimental evidence of flights by measuring tracer particles in a rotating tank with a counter-rotation between inner and outer cylinders. A weak jet pumped fluid through inlets arranged in a ring around the bottom of the tank and generated shear, while outlets around a larger diameter maintained constant fluid volume. The design kept turbulence at a minimum, yet chaotic flows were observed linking together a vortex chain. Figure 6 (left) shows tracer paths and azimuthal angle against time [8]. As in theoretical Levy walks, flights connect the various vortices where particles then mingled for an extended time. Their proxy for diffusion was tracer step variance, which was related to time by an exponent. In the chaotic flow, they measured $\sigma^2 \sim t^\gamma$ where $\gamma = 1.5-1.8$, indicative of anomalous, super-diffusion [8]. Weak turbulence was introduced during a later experiment by changing the fluid injection, and classical diffusion returned, $\sigma^2 \sim t$, or $\gamma = 1$ (Figure 6, right) [8].

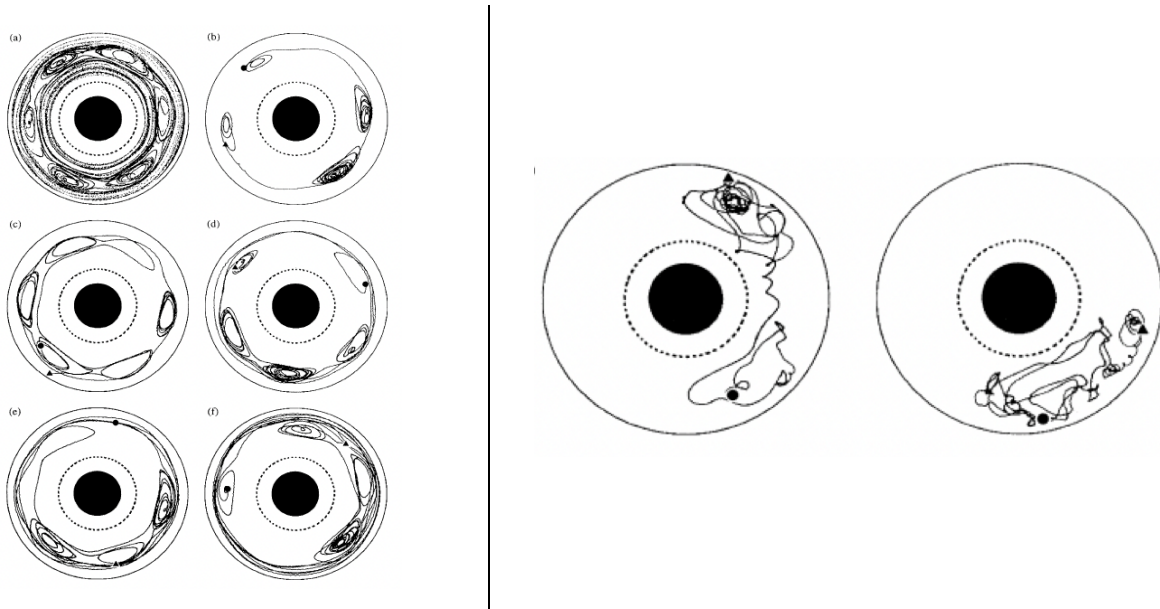


Figure 6 - a) 40 particles after 90 sec, b-f) individual particles from 800 to 1500 sec during sheared, laminar flow (left). Individual particles during weak turbulence (right) [8]

3 Continuous Time Random Walk

Two techniques for dealing with Levy-stable distributions and anomalous diffusion will be elaborated herein, beginning with Continuous Time Random Walks (CTRW). Fokker-Planck (F-P) theory requires a distribution of Δx and can be generalized to allow a distribution for Δt , the system “clock”. Doing so removes locality and Markovian constraints from F-P thereby introducing a more physically representative model. Transitioning to non-Markovian processes corresponds to Kubo number, from previous lectures, larger than unity. CTRW can be implemented by either a waiting time or velocity model, each having strengths and weaknesses. These methods are crudely depicted in Figure 7 [9].

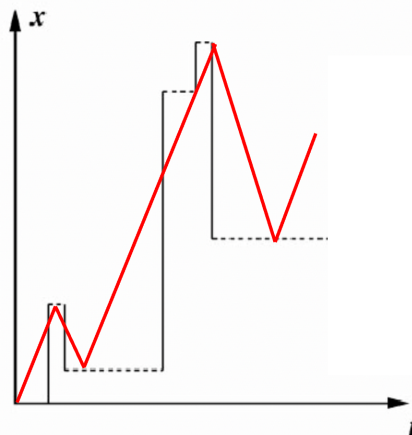


Figure 7 - Rough depiction of Waiting Time (black) and Velocity (red) models [9]

For reference, a short review of F-P will be provided. The Chapman-Kolmogorov equation (CKE) from earlier can be adapted for explicit time dependency as follows

$$P(x, t + \Delta t) = \int d\Delta x P(x - \Delta x, t)P(x|x - \Delta x, t) \quad (3.0.1)$$

Setting $P(x - \Delta x, t) = P$ and $P(x|x - \Delta x, t) = T$ then expanding,

$$P(x, t) + \Delta t \frac{\partial P}{\partial t} = \int d\Delta x \left[PT - \frac{\partial \Delta x PT}{\partial x} + \frac{1}{2} \frac{\partial^2}{\partial x^2} \Delta x^2 TP \right] \quad (3.0.2)$$

There are three key pieces:

$$\int d\Delta x T = 1 \quad (\text{Law of Total Probability}) \quad (3.0.3a)$$

$$\int d\Delta x \frac{\Delta x T}{\Delta t} = V \quad (\text{Drift Velocity}) \quad (3.0.3b)$$

$$\int d\Delta x \frac{\Delta x^2 T}{2\Delta t} = D \quad (\text{Diffusion}) \quad (3.0.3c)$$

Finally, we arrive at the irreversible F-P equation, or FPE,

$$\frac{\partial P}{\partial t} = - \frac{\partial}{\partial x} \left(VP + \frac{\partial DP}{\partial x} \right) \quad (3.0.4)$$

3.1 Waiting Time Model

The waiting time model (WTM) resolves infinite variance in spatial steps by pairing large spatial steps with large time increments. A particle essentially sticks at a position then jumps some Δx at infinite speed leading to the name “leaper”. Each distribution follows

$$\vec{x}_n = r_o + \sum_{i=1}^n \vec{\Delta x}_i \quad (3.1.1a)$$

$$t_n = t_o + \sum_{i=1}^n \Delta t_i \quad (3.1.1b)$$

and the PDF can be factored if they are independent,

$$P(\Delta x, \Delta t) = P(\Delta x)P(\Delta t) \quad (3.1.2)$$

If $P(\Delta t) = 1$ and $P(\Delta x)$ is normal, the traditional FPE is recovered. Otherwise, expand Δx to lowest order for the probability of finding a particle at position x during time t (i.e. jump point distribution),

$$P(x, t) = \int d\Delta x \int d\Delta t P(\Delta x)P(\Delta t)Q = \int_0^t d\Delta t Q\phi \quad (3.1.3)$$

where ϕ is the probability of a particle reaching x at t after Δt , and $Q = P(x, t - \Delta t)$, which is the probability of the particle waiting at its position for Δt . Putting ϕ in terms of the probability that the particle jumps after an interval Δt , $\psi(t)$, and solving for $P(x,t)$,

$$\phi(\Delta t) = \int_{\Delta t}^{\infty} dt' \psi(t') \quad (3.1.4a)$$

$$P(x, t) = \int_0^t d\Delta t \phi Q \quad (3.1.4b)$$

but $\psi(t')$ needs definition by assumption or experiment. This approach lends well to $H < 0.5$, or sub-diffusive systems, due to its built in “sticking” probability where a particle may not jump for large Δt .

Montroll and Weiss pushed the WTM further in 1965 using integral transforms to simplify the involved probabilities [10]. Combining Fourier and Laplace transforms on $P(x,t)$ with N discrete steps and separability results in the Montroll-Weiss equation (MWE),

$$P(k, s) = \sum_{N=0}^{\infty} P(N, s)P_n(k) \quad (3.1.5a)$$

$$P(k, s) = \frac{1 - \psi(s)}{s} \left[\sum_{N=0}^{\infty} \psi(s)P(k) \right]^N \quad (3.1.5b)$$

$$P(k, s) = \frac{1 - \psi(s)}{s} \left[\frac{1}{1 - \psi(s)P(k)} \right] \quad (3.1.4c)$$

$$P(x, t) = \frac{1}{(2\pi)^2 i} \int_{-i\infty}^{c+i\infty} ds \frac{e^{st}}{s} [1 - \psi(s)] \int_{-\infty}^{\infty} dk \left[\frac{e^{-ikx}}{1 - \psi(s)P(k)} \right] \quad (3.1.4d)$$

This model pertains to queuing theory and other applications where waiting times may be random like traffic flow.

3.2 Velocity Model

Managing super-diffusive systems with CTRW is better accomplished with the velocity model (VM). Rather than a particle making infinitely fast jumps, VM relates the time step to spatial increment via a constant travel velocity,

$$P(\Delta x, \Delta t) = \delta\left(\Delta t - \frac{\Delta x}{V}\right) P(\Delta x) \quad (3.2.1)$$

which goes into the CK equation as before,

$$P(x, t) = \int_{-Vt}^{Vt} d\Delta x \int_0^t P(x - \Delta x, t - \Delta t) \Phi_v(\Delta x, \Delta t) \quad (3.2.2a)$$

$$\Phi_v(\Delta x, \Delta t) = \frac{1}{2} \delta(|\Delta x| - V\Delta t) \int_{|\Delta x|}^{\infty} dx' \int_{\Delta t}^{\infty} dt' P(x') \delta\left(t' - \frac{|x'|}{V}\right) \quad (3.2.2b)$$

Φ_v is probability of making a step that at least covers $|\Delta x|$ given velocity V , and $P(x')$ needs definition by assumption or experiment. Insight into the characteristic velocity is also valuable.

Levy flights work well with VM by requiring larger Δx is accompanied by larger Δt through a space-time memory coupling, so this representation may also be called a Levy walk. VM could be called the study of “creepers” due to these properties. Doing so secures a finite variance at a particular step while allowing infinite variance on the steps themselves. Notice as both step variables approach zero in (3.2.2) normal diffusion is recovered.

4 Fractional Kinetics

A second method for managing anomalous diffusion ($\langle \Delta x^2 \rangle \sim t^\gamma, \gamma \neq 1$) is fractional kinetics (FK). In one scenario, $\gamma = \beta/\alpha$ where α and β are non-integers relating $\partial_t \rightarrow \partial_t^\alpha$ and $\partial_x \rightarrow \partial_x^\beta$. FK is most valuable in rough, fractal, and turbulent phase spaces with divergent second moments. Again, there are distributions of step variables, and a non-Markovian process is necessary. Kolmogorov turbulence is one example of this fractional dependence.

FK theory may have been motivated by anomalous diffusion in Taylor and Chirkov’s Standard Map (SM) describing a periodically kicked rotor with angular momentum and angle,

$$p_{n+1} = p_n + K \sin(\theta_n) \quad (4.0.1a)$$

$$\theta_{n+1} = \theta_n + p_{n+1} \quad (4.0.1b)$$

respectively. K is the kick strength, and the remaining parameters are modulo 2π for a torus. Beyond K_{crit} chaotic transport, a form of anomalous diffusion, ensues. The kicked rotor is analogous to a particle in an electric field, so $dv/dt = qE/m$ and K corresponds to $|E|$. A diffusion coefficient comes out of Vlasov plasma quasilinear theory and equals $K^2/2$ in the SM, while the actual diffusion coefficient is $D = \langle (\theta_{n+1} - \theta_n)^2 \rangle$ for large n . The SM phase space and quasilinear-normalized diffusion, $2D/K^2$, are shown in Figure 8 [10].

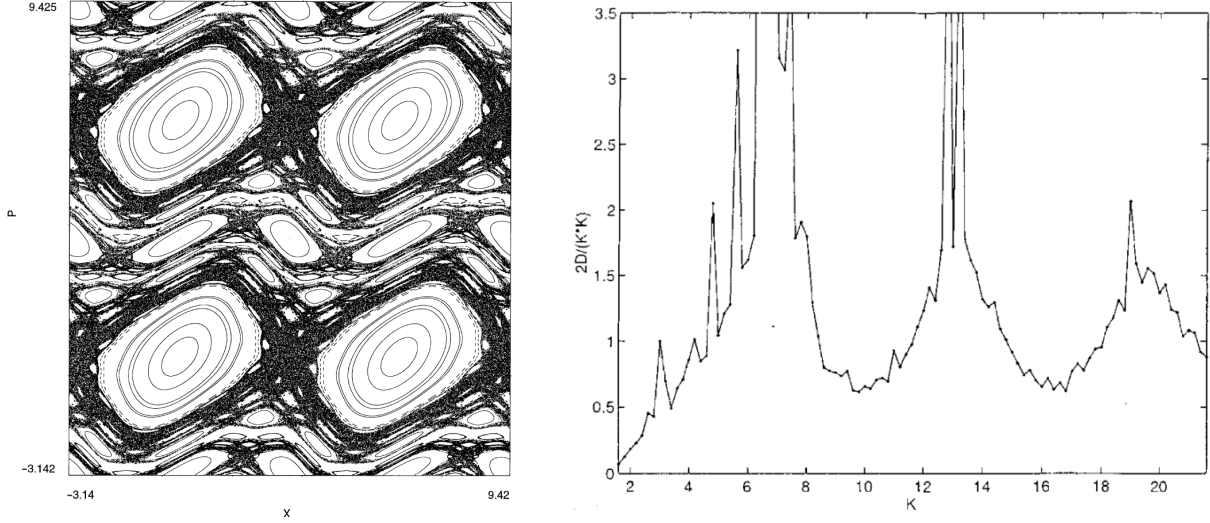


Figure 8 - Taylor-Chirikov Standard Map Phase Space Portrait (left). Normalized diffusion of Standard Map demonstrating accelerator modes as erratic spikes (right). [10]

Previous concepts from this course appear in the Standard Map, namely fixed-point instabilities, resonance overlapping, and stochastic transport. A new idea in SM anomalous diffusion is the accelerator mode, which appears as a spike in the diffusion plot. These accelerator modes are localized but create long time correlations and dominate transport because particles travel along phase space island boundaries. Each accelerator mode has a K in the range $2\pi m \leq K \leq 2\pi m + \Delta K(m)$ related to flights where $\Delta K(m)$ is the phase space island's width and m is an integer. Before going further, an introduction to fractional calculus is needed. The fractional kinetic equation (FKE), which is a generalized form of FPE, can be derived afterwards.

4.1 Fractional Calculus Basics

For integration of order β in time over $f(t)$ where $\beta > 0$, the Cauchy formula extends to

$$I_{\beta}f(t) = \frac{1}{\Gamma(\beta)} \int_{-\infty}^t f(t')(t-t')^{\beta-1} dt' \quad (4.1.1a)$$

$$I_{\beta}f(-t) = \frac{1}{\Gamma(\beta)} \int_t^{\infty} f(t')(t'-t)^{\beta-1} dt' \quad (4.1.1b)$$

which utilizes the gamma function, Γ . These are the Reimann-Liouville integrals. Inversely, $I_{\beta} = \frac{d^{-\beta}}{dt^{-\beta}}$, so the Reimann-Liouville derivatives are,

$$\frac{d^{\beta}f(t)}{dt^{\beta}} = I_{-\beta}f(t) = \frac{1}{\Gamma(n-\beta)} \frac{d^n}{dt^n} \int_{-\infty}^t f(t')(t-t')^{-\beta+n-1} dt' \quad (4.1.2a)$$

$$\frac{d^\beta f(t)}{d(-t)^\beta} = I_{-\beta} f(-t) = \frac{-1}{\Gamma(n-\beta)} \frac{d^n}{d(-t)^n} \int_t^\infty f(t')(t'-t)^{-\beta+n-1} dt' \quad (4.1.2b)$$

where n is the integer part of β . Several useful properties exist in fractional calculus such as

$$\frac{d^{\alpha+\beta}}{dt^{\alpha+\beta}} = \frac{d^\alpha}{dt^\alpha} \frac{d^\beta}{dt^\beta} = \frac{d^\beta}{dt^\beta} \frac{d^\alpha}{dt^\alpha} \quad (4.1.3a)$$

$$\frac{d^\alpha}{dt^\alpha} t^\beta = \frac{\Gamma(1-\beta)}{\Gamma(1+\beta-\alpha)} t^{\beta-\alpha} \rightarrow \frac{d^\alpha}{dt^\alpha} 1 = \frac{t^{-\alpha}}{\Gamma(1-\alpha)} (t > 0) \quad (4.1.3b)$$

$$\lim_{\alpha \rightarrow 1} \frac{d^\alpha}{dt^\alpha} 1 = \delta(t) \quad (4.1.3c)$$

$$F \left\{ \frac{d^\alpha}{d\pm t^\alpha} g(t) \right\} = (\pm ik)^\alpha g(k) \quad (4.1.3d)$$

See [9] for more details on fractional integrals and derivatives.

4.2 Fractional Kinetic Equation

The goal here is to derive an FP-like formulation applicable to anomalous kinetics using fractional calculus. Given a transition probability that a particle moved from (x,t) to $(y,t+\Delta t)$, $W(x,y;t+\Delta t)$, the shift in probability for infinitesimal Δt is to lowest order,

$$\frac{\partial^\beta W(x,y;t)}{\partial t^\beta} = \frac{\partial^\beta P(x,t)}{\partial t^\beta} \quad (0 \leq \beta \leq 1) \quad (4.2.1)$$

where β relates to local temporal fractality. Then, by CKE and dropping higher order terms, the spatial probability shift depends on local phase space fractal dimension parameters, α ,

$$\frac{\partial^\alpha P(x,t)}{\partial x^\alpha} (\Delta t)^\alpha = \Delta_x^\alpha P(x,t) = \int dy [W(x,y;t+\Delta t)P(y,t)] - P(x,t) \quad (4.2.2)$$

and probability conservation requires

$$\frac{\partial^\alpha P(x,t)}{\partial x^\alpha} \approx \frac{\partial^\beta P(x,t)}{\partial t^\beta} \quad (4.2.3)$$

Applying limits in Δt shows,

$$\frac{\partial^\beta P(x,t)}{\partial t^\beta} = \lim_{\Delta t \rightarrow 0} (\Delta t)^{-\beta} \int dy [W(x,y;t+\Delta t)P(y,t)] - P(x,t) \quad (4.2.4)$$

Now an expression for W is needed, which begins with expansion in $\Delta t \rightarrow 0$,

$$W(x, y; \Delta t) = \delta(x - y) + A(y, \Delta t)\delta^\alpha(x - y) + B(y, \Delta t)\delta^{\alpha_1}(x - y) \quad (4.2.5)$$

($0 \leq \alpha \leq \alpha_1 \leq 2$) – Levy Index Constraint

where a $\frac{1}{2}$ is wrapped into B . An assumption of temporal locality must be made to resolve A and B independent of $P(x, t)$. Using moments of W to solve B ,

$$\langle |\Delta x|^{\alpha_1} \rangle = \int dx |x - y|^{\alpha_1} W = \alpha_1! B(y, \Delta t) = \Gamma(1 + \alpha_1) B(y, \Delta t) \quad (4.2.6)$$

The gamma function results from repeated integration by parts, which also eliminates A ($\alpha \leq \alpha_1$). To find A , integrate (4.2.5) over y ,

$$\int dy W = 1 = 1 + \int dy \frac{\partial^\alpha A(y, \Delta t)}{\partial y^\alpha} \delta(x - y) + \int dy \frac{\partial^{\alpha_1} A(y, \Delta t)}{\partial y^{\alpha_1}} \delta(x - y) \quad (4.2.7a)$$

$$\frac{\partial^\alpha A(x, \Delta t)}{\partial (-x)^\alpha} = - \frac{\partial^{\alpha_1} B(x, \Delta t)}{\partial (-x)^{\alpha_1}} \quad (4.2.7b)$$

but in the limit $\Delta t \rightarrow 0$,

$$\frac{\partial^\alpha \hat{A}(x)}{\partial (-x)^\alpha} = - \frac{\partial^{\alpha_1} \hat{B}(x)}{\partial (-x)^{\alpha_1}} \quad (4.2.8a)$$

$$\hat{A}(x) = \lim_{\Delta t \rightarrow 0} (\Delta t)^{-\beta} A(x; \Delta t) \quad (4.2.8b)$$

$$\hat{B}(x) = \lim_{\Delta t \rightarrow 0} (\Delta t)^{-\beta} B(x; \Delta t) \quad (4.2.8c)$$

For reference, (4.2.6-7) have made use of the identity

$$\int dx f(x) \delta^n(x) = (-1)^n \int dx \frac{\partial^n f(x)}{\partial x^n} \delta(x) \quad (4.2.9)$$

Now with (4.2.5) and the recent results, (4.2.4) simplifies to a result resembling the typical FPE,

$$\frac{\partial^\beta P(x, t)}{\partial t^\beta} = \lim_{\Delta t \rightarrow 0} (\Delta t)^{-\beta} \int dy [W(x, y; \Delta t) - \delta(x - y)] P(y, t) \quad (4.2.10a)$$

$$\frac{\partial^\beta P(x, t)}{\partial t^\beta} = \frac{\partial^\alpha}{\partial (-x)^\alpha} \hat{A}(x) P(x, t) + \frac{\partial^{\alpha_1}}{\partial (-x)^{\alpha_1}} \hat{B}(x) P(x, t) \quad (4.2.10b)$$

(4.2.10b) is the Fractional Kinetics Equation (FKE) with critical exponents α, α_1, β . The critical exponents can be determined with experimental data or additional information relating the system to “prototype” universality classes.

Setting $\alpha_1 = \alpha + 1$, the FKE simplifies to a “fractional Fick’s Law”,

$$\frac{\partial^\beta P(x, t)}{\partial t^\beta} = - \frac{\partial^\alpha}{\partial (-x)^\alpha} \hat{B}(x) \frac{\partial P(x, t)}{\partial x} \quad (4.2.11)$$

The special cases stemming from this are,

$$\text{FPE} \quad \alpha = \beta = 1 \quad (4.2.12a)$$

$$\text{Fractional Brownian} \quad \alpha = 2, \quad 0 < \beta < 1 \quad (4.2.12b)$$

$$\text{Levy Process} \quad 1 < \alpha < 2, \quad \beta = 1 \quad (4.2.12c)$$

Physically, A controls convection, while B controls diffusion, which is obvious given the above conditions. System observables correspond to moments describing global evolution, i.e.

$$\langle |x|^\gamma \rangle = \int dx |x|^\gamma P(x, t) \quad (4.2.13)$$

For a slowly varying A and negligible B, moments from the FKE can be obtained:

$$\frac{\partial^\beta}{\partial t^\beta} \langle |x|^\alpha \rangle = A \int dx |x|^\alpha \frac{\partial^\alpha P(x, t)}{\partial t^\alpha} = \alpha! A \int dx P(x, t) = \Gamma(1 + \alpha) A \quad (4.2.14a)$$

$$\langle |x|^\alpha \rangle = A t^\beta \Gamma(1 + \alpha) / \Gamma(1 + \beta) \quad (4.2.14b)$$

If the dynamics are self-similar one expects $\langle |x| \rangle = t^{\beta/\alpha} = t^{\mu/2}$ where $\mu = 2\beta/\alpha$. This ratio of critical exponents denotes an extension from standard diffusion. The variance with time is then $\langle |x|^2 \rangle = t^\mu$, so anomalous diffusion is possible in the FK approach. Thinking back to the SM, one might guess phase space structure has something to do with this. Going further back, one might also notice a relation between FK and the Hurst parameter. These natural connections have led to a growing number of FK applications with strong memory effects including polymer deformation, semiconductor trapping, and tokamak transport. A final comment on FK is how it compares with FP beyond (4.2.12a), which Table 1 summarizes.

4.3 Weierstrass Random Walk

The final topic relating to FK is the Weierstrass Random Walk (WRW) developed by Hughes, Shlesinger, and Montroll in 1981 [12]. Conceptually, it falls between a CTRW and FK, but the WRW explicitly depends on self-similarity of scale and fractal motion, so describing it alongside FK works well. The Weierstrass function itself is continuous everywhere but differentiable nowhere, or in other words, rough. Starting with a periodic, 1D lattice with nodes on unit length integers, define a probability to achieve position l in terms of the probability p_j to make a step of length a_j ,

Table 1 - Summary of differences between Fokker-Planck and Fractional Kinetic Theories

	FP	FKE
Derivatives	∂_x, ∂_t	$\partial_x^\alpha, \partial_t^\beta$
Stochastic variable	Δx	$\Delta x, \Delta t$
Time	Fixed	Variable with PDF
Second Moment scaling	$\langle x ^2 \rangle \propto t$	$\langle x ^2 \rangle \propto t^\mu, \mu \in (0, 2)$
Kolmogorov Conditions	$\lim_{\Delta t \rightarrow 0} \frac{1}{\Delta t} \langle \langle \Delta x \rangle \rangle = \mathcal{A}(x)$ $\lim_{\Delta t \rightarrow 0} \frac{1}{\Delta t} \langle \langle (\Delta x)^2 \rangle \rangle = \mathcal{B}(x)$ $\lim_{\Delta t \rightarrow 0} \frac{1}{\Delta t} \langle \langle (\Delta x)^m \rangle \rangle = 0; m > 2$	$\lim_{\Delta t \rightarrow 0} \frac{A(x, \Delta t)}{(\Delta t)^\beta} = \mathcal{A}(x)$ $\lim_{\Delta t \rightarrow 0} \frac{B(x, \Delta t)}{(\Delta t)^\beta} = \mathcal{B}(x)$
$A(y, \Delta t)$	$\langle \langle (\Delta y) \rangle \rangle$	-
$B(y, \Delta t)$	$\langle \langle (\Delta y)^2 \rangle \rangle$	$\frac{\langle \langle \Delta x ^{\alpha_1} \rangle \rangle}{\Gamma(1+\alpha_1)}$
$\mathcal{A}(x)$ to $\mathcal{B}(x)$ relation	$A(y, \Delta t) = \frac{1}{2} \frac{\partial B(y, \Delta t)}{\partial y}$	$\frac{\partial^\alpha \mathcal{A}(x)}{\partial (-x)^\alpha} = - \frac{\partial^{\alpha_1} \mathcal{B}(x)}{\partial (-x)^{\alpha_1}}$

$$P(l) = \frac{1}{2} \sum_{j=1}^{\infty} [\delta(l - a_j) + \delta(l + a_j)] \quad (4.3.1a)$$

$$P(l) = \int_{-\infty}^{\infty} dl P(l) = 1 \quad (4.3.1b)$$

Two delta functions appear due to an assumed symmetry in the walk. Now, assume only exponential stepping and set a normalization constant to emphasize large scale behavior,

$$a_j = a^j, \quad p_j = Cp^j, \quad C = 1 - p \quad (4.3.2)$$

Substituting into (4.3.1a) and solving for the characteristic Weierstrass function by Fourier transform yields,

$$P(l) = \frac{1}{2} (1 - p) \sum_{j=1}^{\infty} p^j [\delta(l - a^j) + \delta(l + a^j)] \quad (4.3.3a)$$

$$P(k) = (1 - p) \sum_{j=0}^{\infty} p^j \cos(ka^j) \quad (4.3.3b)$$

The second moment of $P(l)$, $\langle l^2 \rangle$, is of note because it diverges if $a^2 p \geq 1$. $P(k)$ satisfies

$$P(k) = pP(ka) + (1 - p)\cos(k) \quad (4.3.4)$$

which resembles the renormalization group equation (RGE) and suggests the solution

$$P(k) = P_s(k) + P_r(k) \quad (4.3.5)$$

where $P_s(k)$ is a singular part and $P_r(k)$ is a regular part. By renormalization,

$$P_s(k) = pP_s(ak) \quad (4.3.6)$$

becomes singular for $k \rightarrow 0$,

$$P_s(k) \approx |k|^\mu Q(k) \quad (4.3.7)$$

$Q(k)$ is some non-singular function at small k and μ is an exponent related to the Levy index. Substituting (4.3.7) into (4.3.6) we find a relation between step probability and step size,

$$\mu = -\ln(p)/\ln(a), \quad \ln(p) < 0 \quad (4.3.8)$$

Self-similarity thus appears due to the scaling assumptions and a connection to previous content, especially the relation between Levy index and the random walk, is evident. Much more could be said about the WRW, but the key points have been elucidated.

5 References

- [1] Mandelbrot, B.B., Wallis, J.R. (1968). *Water Resources Research*, **4**, 909.
- [2] Mandelbrot, B.B., Ness, J.W. (1968). *SIAM Review*, **10**, 422.
- [3] Hurst, H.E. (1951). *Transactions of the American Society of Civil Engineers*, **116**, 2447.
- [4] Thomas, V., Wang, Y., Xibo, F. (2001). *Policy Research Working Paper*, **2525**.
- [5] Doyle, J.A., Evans, A.C. (2018). *arXiv:1806.03704v1*.
- [6] <https://www.mathworks.com/help/stats/stable-distribution.html>
- [7] Zamli, K.Z., Din, F., et al. (2018). *arXiv:1805.00873v1*.
- [8] Solomon, T.H., Weeks, E.R., Swinney, H.L. (1993). *Physical Review Letters*, **71**, 3975.
- [9] Metzler, R., Klafter, J. (2000). *Physics Reports*, **339**.
- [10] Zaslavsky, Z.M. (2002). *Physics Reports*, **371**.
- [11] Samko, S.G., Kilbas, A.A., Marichev, O.I. (1993). *Fractional Integrals and Derivatives: Theory and Applications*. CRC Press, Boca Raton, FL.
- [12] Hughes, B.D., Schlesinger, M.F., Montroll, E.W. (1981). *Proceedings of the National Academy of Sciences of the United States of America*, **78**, 3287.